Reliability of Bi-stable Single Domain Nano Magnets for Cellular Automata

Javier F. Pulecio, *Student Member*, *IEEE*, Sanjukta Bhanja, *Member, IEEE*

***Abstract*—Quantum Cellular Automata, also known as QCA, has been touted as a pragmatic use of quantum phenomena which currently are detrimental in nano-transistor technology. Recently, QCA technologies has expanded into magnetism [1][2], an area referred to as Magnetic QCA, by exploiting the magnetic coupling interaction between neighboring cells (nano-magnets). The interactions of orderly fabricated nano-magnets and the viability of nano-magnetic structures as logical building blocks has yet to be explored in great detail. We have fabricated nano-scale Magnetic QCA cells and currently the scope entails determining how factors such as material, size, placement, and surface roughness affect the magnetic properties and coupling interactions between the nano-magnetic QCA cells.**

I. Introduction

CMOS technology has often defied pessimistic predictions of scaling but most agree that there exist a physical limitation to the reduction of feature sizes in the CMOS transistor. As a result Chemist, Engineers, and Physicist are exploring the various technologies to succeed the CMOS transistor. This does not imply that CMOS will not be a part of the future; instead many believe that the next generation of digital devices will be a hybrid of CMOS and it's successor. HP's crossbar latch, photonic crystals, carbon nano-tube transistors, Y-junction carbon nano-tubes, single electron transistors, magnetic domain walls, molecular chains, and quantum cellular automata are a few of the nano-scale technologies that could be the next "Lego" in logic devices. Here we present what has been realized in Magnetic QCA, what we have accomplished, and our future objectives.

II. What Is QCA?

In cellular automata, a basic cell has distinct enumerated states which are determined by its current state and the state of its neighbors. These cells are positioned in such a fashion that direct neighbors will influence and change each others current state. A good example of cellular automata is John Conway's Game of Life. Quantum Cellular Automata, or QCA, is a flavor of cellular automata in which the intrinsic and extrinsic properties of the cell(s) are based on the quantum effects of an electron(s). An interesting fact of QCA is that it is not limited to a specific quantum phenomenon; meaning that there are several physical implementations of a QCA cell which embody the electron differently and make use of distinct quantum effects. Currently, there are three prominent breeds of QCA; Magnetic, Electronic, and Molecular.

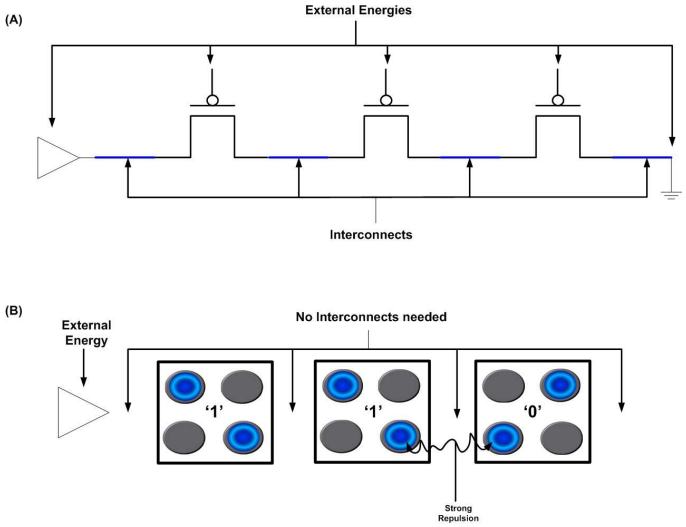

Fig. 1. (A) is a very simple diagram of transistors in series which depicts various external energies and interconnecting wires which are not necessary for QCA. It is also important to note that the transistors require a constant energy supply to operate which is not the case for QCA. (B) is a non-specific QCA implementation of a QCA wire. The leftmost cell can be considered a state of '1' and the rightmost cell state '0'. The external source has forced the leftmost cell to change it's state to '1' and this cell has forced the neighboring middle cell to also change to a '1'. The last rightmost cell, which is a '0', will also eventually change to '1' because of the coupling force experienced from its neighboring cell.

The beauty of QCA is that each cell is a self contained element, needing no external energy to maintain a state. The desired state will always be one of the possible energy minimum configurations of the cell. There is no need for constant power to operate the QCA system, external energy is only provided during switching of states, making QCA an inherently low power system. Another excellent characteristic of QCA is that it is a lead-less system, meaning there is no

Manuscript sent May 31, 2007. This work is supported by the NSF FGLSAMP Bridge to Doctorate supplement award GEO# 0503536.

Javier F. Pulecio is with the Department of Electrical Engineering at the Unviersity of South Florida, Tampa, FL, 33620 USA, phone: 813-974-4477, fax: 813 974 5250, email: jpulecio@eng.usf.edu

Sanjukta Bhanja is with the Department of Electrical Engineering at the Unviersity of South Florida, Tampa, FL, 33620 USA, phone: 813 974 4755, fax: 813 974 5250, email: bhanja@eng.usf.edu

need for physical interconnects between all of the QCA cells. Cells interact with neighbors via cell coupling forces which depend on the particular QCA schema. This significantly reduces the already stringent requirements to fabricate any real nano-scale device. **Figure 1** depicts a very generic comparison of transistor and QCA technologies. Thus far, of the various QCA schema, only Magnetic QCA has been able to demonstrate successful operation at room temperature [1][2].

III. Magnetic QCA

In Magnetic QCA, a basic cell is a nano magnet; these magnetic cells are arranged in various grid-like fashions to accomplish computing. Cells in Magnetic QCA are enumerated based on their single domain magnetic dipole moments and are inherently energy minimums. The single domain phenomenon only occurs in nano-scale magnets and its significances lies in the fact that it reduces the cell's coercivity. This enables lower magnetic fields to alter the cells magnetic moments and thus providing the desired switching characteristics. Two distinct and significant advancements in Magnetic QCA have been made which we will summarize in following subsections.

A. Magnetic QCA Dots

In this scheme, Cowburn et al. constructs a network by placing an elongated elliptical input dot followed by circular dots which form a wire as shown in **Figure 2** [1]. The elliptical input dot requires a greater magnetic field to change states than that of the circular dots, due to the shape anisotropy. Once the state of the input dot has settled, it is propagated down the circular QCA wire. The input dot state is set to a logical '1' or '0' by applying a single magnetic field pulse along the wire of dots at +300 Oe (returning to 0 Oe) or -300eV (returning to 0 Oe), respectively. To ensure that the magnetic pulse used to set the input dot did not set the circular dots states as well, the same magnetic pulse of ±300 Oe was sent along the wire without the input dots present. The dipole moments of the circular Nanodots were not uniformly aligned to the external field, hence ensuring the propagation of a state was due to the magnetostatic coupling forces and not the external field applied to set the input dot. A weak oscillating magnetic field of ±25 Oe at a 30Hz frequency, combined with a -10 Oe bias magnetic field is also applied to the entire network of dots to propagate the state of the input dot down the wire of circular

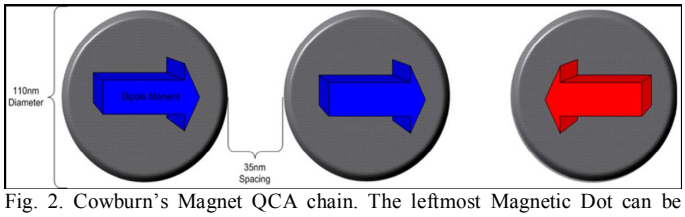

Fig. 2. Cowburn's Magnet QCA chain. The leftmost Magnetic Dot can be assumed to be a logical '1', while the rightmost can be assumed to be a logical '0'. In this wire, the two leftmost Magnetic Dots have coupled which represents state or informational propagation. The final dot which has a state of '0' will soon change to '1' to minimize local magnetic energies.

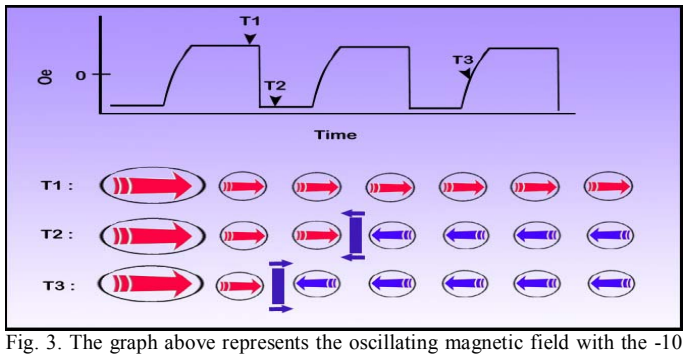

Fig. 3. The graph above represents the oscillating magnetic field with the -10 Oe bias. At time T1 the majority of the wire has followed suit with the input dot. At T2 the negative phase of oscillation combined with the bias has sufficient energy to reverse the state of the wire by propagating a soliton down the wire one by one. T3 has the soliton moving forward along the chain as it enters the positive phase of oscillation.

dots. To propagate or reverse the state of the network a soliton is created [1]. Once created, usually near the end of the QCA wire, the soliton can move back and forth along the chain depending on the magnetic oscillating field. **Figure 3** depicts how the propagation of states could occur. Note at T2, when the soliton reaches the input dot it will stay between the input dot and the first circular Nanodot. Once the magnetic oscillating field begins to rise the soliton will begin to move foward along the chain, as depicted at T3. Had the input dot been set to 0 (magnetic dipole moment pointing to the left) and the soliton moving backward, as depicted at time T2, the soliton would be lost and another would need to be created.

In the network described above the circular dots were fabricated to a diameter of 110 nm, a thickness of 10 nm, at a pitch of 135nm as shown in **Figure 2**. The size and shape ensured that the ferromagnetic circular dots, made of a Supermalloy $Ni_{80}Fe_{14}Mo_5X_1$ where X is other metals, have only a single domain. This is important when considering the hysteresis phenomenon experienced by multiple domain magnets. It was found that the circular dots with a diameter of 100 nm and thickness of 10 nm exhibited ideal switching characteristic [4]. The minute amount of energy required to saturate the dot, starting at about 5 Oe, and the high residual magnetization, about 80%, are prime characteristics that are produced by these single domain dots [4]. The magnetostatic energy (PE in the magnetic field) between two dots in this network is about 200 k_bT, where k_b is the Boltzmann's constant and T is the temperature, and it should be at least 40 k_bT to keep thermal errors below one per year [4].

B. Field-Coupled Nanomagnets

In Csaba's et al. network, the basic cell consist of a magnetic single domain nano pillar shown in **Figure 4(A)**. Due to the shape anisotropy, the pillars develop easy and hard axises as shown in **Figure 4(B&C)**. When aligned along the easy axis the pillars experience less demagnetization energy and hence are in an energtically favorable state. Therefore, when aligned

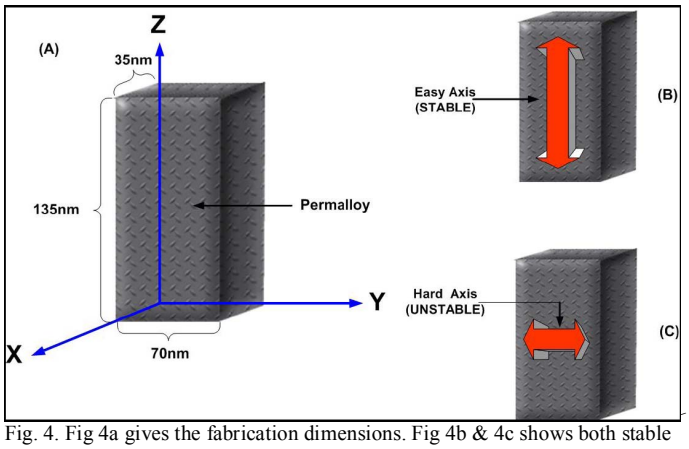

Fig. 4. Fig 4a gives the fabrication dimensions. Fig 4b & 4c shows both stable and unstable configurations of magnetic moments in the absence of an external magnetic field. The state in Fig 4c is undesired because the dipole moment experiences higher demagnetization energies and will eventually align along the easy axis either point upward or downward.

along the hard axis, the magnetic dipole moment is unstable and will eventually align itself along the easy axis to reduce the demagnetization energy. A Magnetic QCA wire is construct by placing nano pillars side by side as shown in Figrue 5(A). In this network, proper data propagation occurs when all magnets in the QCA wire are antiparallel to each other. Let's assume the wire's initial state in **Figure 5(A)**, which can be anything, is the entire chain's dipole moment pointing upward along the Z-axis. Csaba et al. suggest an "adiabatic pumping" scheme [5] where the energy barrier required for an input to overcome is reduced by first applying a magnetic field along the Y-axis. This causes the Nanopillar's dipole moment to align itself along the hard axis. This state is energitically unfavorable, making it possible to supply a weaker external magnetic input field to the system. Once an input is supplied, magnetostatic coupling energies between the magnets causes data to propagate down the wire. **Figure 5(B)** is a Magnetic QCA Majority Gate, which to the best of our knowledge is the first logic gate fabricated in this type of QCA [6][9]. The shape of a rectangular nano pillar seems to be chosen
by Csaba et al. because of their bistable nature. The shape anisotropy of the Nanopillars introduces a high energy barrier between the two stable states thereby making them less error prone. This high energy barrier also leads to power dissapation but Csaba et al. mitigates this by introducing a type of adiabatic switching/pumping mentioned previously. The Nanopillars fabricated by Csaba et al. have a thickness of 35nm, width of 70nm, height of 135nm, and are made of a permalloy [6]. The Nanopillars are fabricated in a similar Electron Beam Lithography process as Cowburn et al. [6]. Csaba et al. also appears to be the first to demonstrate modeling of single domain magnets in SPICE [2].

We are particularly interested in Csaba's *et al.*[2] implementation of nano-magnets due to there bi-stable nature. The shape anisotropy significantly reduces meta-stable states, which in turn allows stronger coupling between neighboring nano-magnetic cells. Our desire here is to characterize the

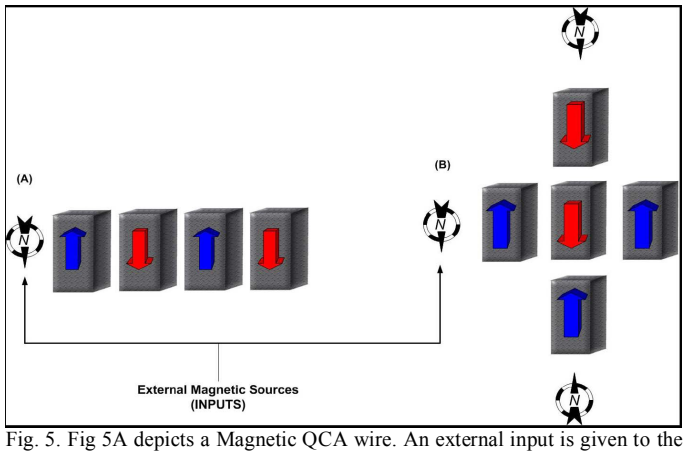

Fig. 5. Fig 5A depicts a Magnetic QCA wire. An external input is given to the wire which has sufficient strength to coerce the rest of the wire to change its state accordingly. Note that regardless of the previous state of the wire the result will be as shown. Fig 5b is a Magnetic QCA Majority Gate. This has three inputs given to the gate, the result will depend on the dipole moments of the inputs. In this example the topmost and leftmost inputs have the north end of the dipole moment pointing downward and the bottom input has it's mo ment pointing upward. The majority of the inputs are pointing downward so the center pillar is the result of the majority.

reliability of both the individual cell's magnetic moment and magnetic coupling of neighbors. We begin by analyzing simple chains of the nano-magnetic cells in hopes to be able to use them as interconnects for more complicated logic.

IV. Fabrication Methods

A. Spinning

The process begins by coating a Si wafer with a resist, namely PMMA. This was accomplished by using a Laurell Technologies WS-400A-8NPP/Lite Spin Processor, which spins the wafer at high speeds causing the PMMA resist to spread evenly over the entire wafer. We chose a bi-layer PMMA recipe using 450A molecular weight as the bottom layer and 950A molecular weight as the top layer. The bottom layer was spun, then baked, followed by the top layer being spun then baked.

B. Lithography and Development

A pattern is designed using DesignCAD2000 NT. The most effective line spacing, exposure doses, points, and focus are determined by using diagnostic wheel pattern. A sample of the Si coated with bi-layer PMMA is then loaded into the JOEL 840m retrofitted with the NPGS lithography system and a beam blanker. The SEM is then focus and the stigmation is adjusted for best results. The pattern is selected and written via the NPGS system. Afterwards, the sample is unload and ready to be developed. It is placed in a bath of MIBK 3:1 for approximately seventy seconds, followed by a twenty second isoproponal bath, and finally nitrogen dried.

C. Deposition and Liftoff

We then deposited the ferromagnetic material of our choice, in this case Nickel, via the Varian Model 980-2462 Electron Beam Evaporator. We achieve a vacuum of about 2 μTorr and

evaporated the material at a rate fast rate to lessen contamination. Once we deposited the desired thickness of our material we preceded to the liftoff step. We placed our sample coated with Nickel in a heated ultrasonic acetone bath for approximately 15 minutes which lift's off the PMMA leaving our magnetic structure intact.

V. Results

Figures 6, **7**, and **8** are a set of images of three different chains of nano magnetic cells and have the following images from top to bottom: a SEM surface image, an AFM 3D surface plot, an AFM surface image, and a MFM image. Each set of images is of the same chain of nano magnetic cells and each cell has the dimensionality of approximately 160nm height x 80nm width x 40nm thickness. The rational is to compare the magnetic moments of each cell and the resulting magnetic coupling of neighbors to; surface roughness, shape regularity, cell spacing, and cell size. Preliminary results show that Nickel does indeed have single domain characteristics parallel to the substrate (in-plane) at dimensions mentioned above as evident **Figures 6**, **7**, and **8**. We also note that magnetic coupling is evident due to the anti-parallel alignment of the cells.

In **Figure 6**, there are several nano magnetic cells with very irregular shapes and uneven surfaces. The AFM images clearly show the surface roughness where the SEM images present the shape irregularities, cell spacing, and cell spatial orientation. Here we see that even if the magnet does not have a uniform shape and neighbors are not completely parallel to one another that single domain magnetic dipole moments still formed and data propagation still occurred, evident via the anti-parallel coupling of cells 5 through 10 (left to right). We point out that cells 1 and 2 had an unwanted coupling state which we attribute to the surface irregularities. We also note that where there are large protrusions on the surface of a cell the magnetic moment seems to be voided as evident in cell 4.

Figure 7 is a different chain of nano magnets. Overall the various cells have a smoother surface and more regular shape than the chain in **Figure 6**. Cells 2 and 4 have large bulges on the surfaces and the MFM image depicts magnet voids in corresponding areas. Cells 2 and 3 are in an undesired configuration, with like orientations of there magnetic moments, which we attribute to the irregular surfaces. We also note that even though cell 1 has a very irregular shape (almost square) it still managed to form a desired single domain magnetic moment.

Figure 8 is an ideally fabricated chain of nano magnetic cells. We see that the shape, surface, spacing, and orientation are better than that of the previous chains mentioned above. We point out that there are no configuration errors in this chain, all magnets are in a anti-parallel orientation and thus propagating information correctly. We mainly attribute this to the surface evenness of the nano magnetic cells.

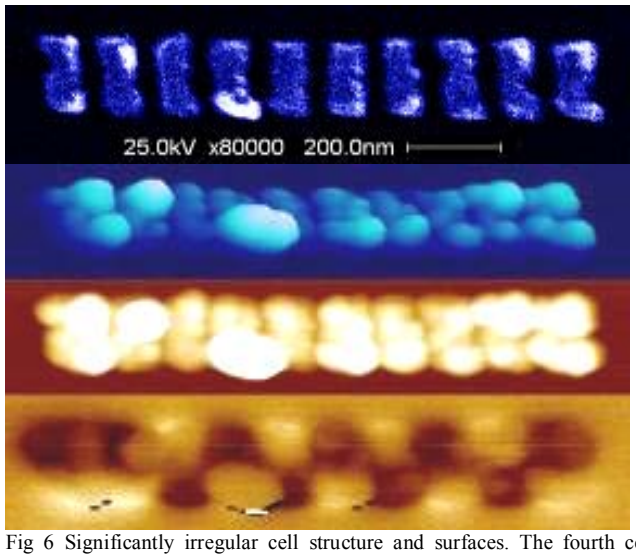

Fig 6 Significantly irregular cell structure and surfaces. The fourth cell from the right has no in-plane moment due to the surface imperfection.

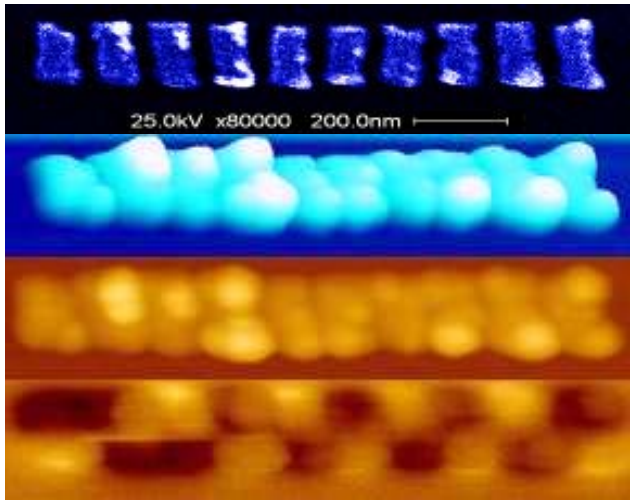

Fig 7 In this chain, cells with a smoother surface have better defined symmetrical dipole moments.

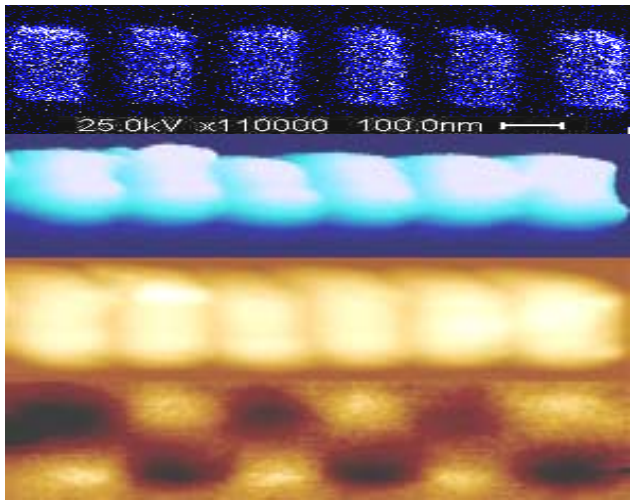

Figure 8 An ideal chain, where the shape of the cells is regular and the surface roughness has been reduced. As a result the single domain dipole moments are strongly coupled.

We conclude that shape uniformity is a much more lenient requirement than that of surface roughness for reliable data propagation. Here we presented several examples were irregularly shaped rectangular nano cells are able to establish a single domain magnetic moments. The irregularly shaped cells are also able to propagate data to neighboring cells which is demonstrated via an anti-parallel magnetic coupling. We also established a relationship between surface roughness and magnetic moments. We note that configuration errors, where neighbors have similar magnetic dipole moment orientations, occur near cells that have irregular surfaces. The reliability of a Magnetic QCA wire therefore relies heavily on the fact the surface must be uniformly smooth in order to propagate data properly.

Currently, we are studying data propagation of longer chains and fabricating majority gates. We are also scaling the magnets in half, as shown in **Figure 6**, and using different ferromagnetic materials to see how this affects the cell properties.

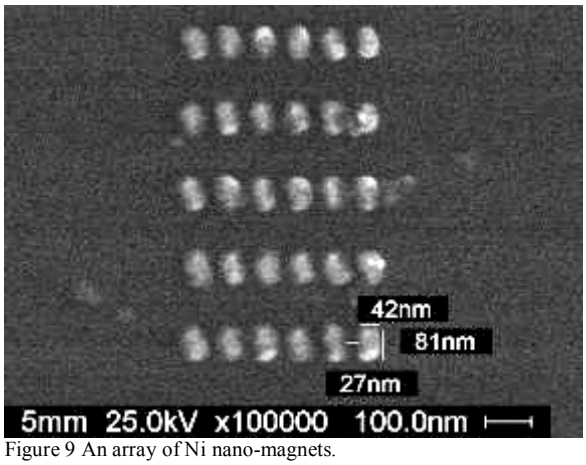

Figure 9 An array of Ni nano-magnets.

REFERENCES

[1] R. P. Cowburn and M. E.Welland, "Room temperature magnetic quantum cellular automata," SCIENCE, vol. 287, pp. 1466–1468, February 2000.

[2] G. Csaba, A. Imre, G. H. Bernstein, W. Porod, and V. Methlushko, "Nanocomputing by field-coupled nanomagnets," IEEE Transactions on Nanotechnology, vol. 1, December 2002.

[3] M. C. B. Parish and M. Forshaw, "Magnetic cellular automata mca systems," IEEE Proc-Circuits Devices Syst., vol. 151, pp. 480–485, October 2004.

[4] R. P. Cowburn, D. K. Koltsov, A. O. Adeyeye, and M. E. Welland, "Single-domain circular nanomagnets," The American Physical Society, vol. 83, pp. 1042–1045, August 1999.

[5] G. Csaba, P. Lugli, and W. Porod, "Power dissipation in nanomagnetic logic devices," IEEE Conference on Nanotechnology, 2004.

[6] A. Imre, G. Csaba, L. Ji, A. Orlov, G. Bernstien, and W. Porod, "Power dissipation in nanomagnetic logic devices," IEEE Conference on Nanotechnology, 2004.

[7] W. J. Gallagher U.S. Patent 5 640 343, 1997.

[8] R. P. Cowburn, "Digital nanomagnetic logic," 2004.

[9] A. Imre, G. Csaba, L. Ji, A. Orlov, G. H. Bernstein,W. Porod "Majority Logic Gate for Magnetic Quantum-Dot Cellular Automata," SCIENCE, vol. 311, January 2006.